JOURNAL OF MATERIALS SCIENCE 16 (1981) 2988–2996

# A microstructural examination of the flow behaviour of a superplastic copper alloy

SHEN-ANN SHEI*, TERENCE G. LANGDON
*Departments of Materials Science and Mechanical Engineering, University of Southern California, Los Angeles, California 90007, USA*

There are important differences in the microstructures of specimens of a superplastic copper alloy deformed in the three regions of flow associated with superplasticity. There is very extensive dislocation activity at high strain rates in Region III, whereas at intermediate and low strain rates in Regions II and I the dislocation density is low and many of the grains appear to be dislocation-free. Measurements show that grain-boundary sliding is important in Region II but decreases in magnitude in the less superplastic Regions I and III.

## 1. Introduction

Many experiments have been conducted to determine the flow properties of materials exhibiting superplasticity, and the significant results are summarized in two recent reviews [1, 2]. In general, superplastic metals tend to exhibit a sigmoidal or three-stage variation between the steady-state flow stress, $\sigma$, and the steady-state strain rate, $\dot{\epsilon}$, thereby dividing the mechanical behaviour into three distinct regions. At low strain rates in Region I, the stress exponent, $n$ ($= \partial \ln \dot{\epsilon} / \partial \ln \sigma$), is high and the tensile elongations to failure are relatively small; at intermediate strain rates in Region II, the stress exponent is low, typically close to 2, and the material exhibits high superplastic elongations; and at high strain rates in Region III, the stress exponent is again high and the fracture elongations are correspondingly reduced.

Despite the large number of investigations of superplasticity conducted to date, there have been relatively few detailed studies of the deformed microstructures using transmission electron microscopy. Naziri *et al.* [3, 4] performed a series of detailed *in situ* experiments on the Zn–22 wt % Al eutectoid alloy in the high-voltage electron microscope. However, these tests were conducted in Region II only and subsequent calculations [5] showed that the results may not be reliable because the diffusivity in the Al-rich grains was probably enhanced by up to five orders of magnitude by irradiation damage from the electron beam. An additional criticism is that the experiments were performed on thin foils which were essentially two-dimensional in character [6], with only approximately one grain in the specimen thickness.

Subsequently, Samuelsson *et al.* [7] conducted a detailed study of the deformed structure of a Zn–40 wt % Al alloy in Regions II and III, Matsuki *et al.* [8] examined a superplastic Al–6 wt % Mg alloy after deformation in Region II, Valiev and Kaibyshev [9] observed the grain-boundary structure of a Mg–1.5 wt % Mn–0.3 wt % Ce alloy deformed in Regions II and III, Kaibyshev *et al.* [10] reported observations on Zn–10 wt % Al and Zn–50 wt % Al after deformation in Regions I, II and III, and Matsuki *et al.* [11] examined two Al–Cu–Zr alloys after deformation in Regions II and III. Very recently, Valiev *et al.* [12] performed *in situ* experiments in the high-voltage electron microscope using a superplastic Zn–0.4 wt % Al alloy deformed at room temperature at a strain rate corresponding to Region II. A notable feature of this brief summary of earlier work is therefore the very limited microscopic data available at present for superplastic materials deformed in Region I at low strain rates.

An additional unresolved problem in super-

*Present address: Metallurgy and Ceramics Division, Ames Laboratory, Iowa State University, Ames, Iowa 50010, USA.



0022–2461/81/112988–9$02.90/0 © *1981 Chapman and Hall Ltd.*

plastic metals concerns the role and magnitude of grain-boundary sliding in superplastic deformation. Although all theories of superplasticity are based on the occurrence and accommodation of sliding, experimental measurements consistently indicate a strain contribution due to sliding of about 50 to 70% in Region II and a sharp decrease in the sliding contributions in Regions I and III [13].

The present experiments were undertaken with two specific objectives. First, to perform a detailed examination of the microstructures in a superplastic metal after deformation in each of the three regions of plastic flow. Second, to take a series of measurements to determine the magnitude of sliding in each of these regions.

The experiments were performed on Coronze CDA 638, a commercial alloy containing 95 wt% Cu, 2.8 wt% Al, 1.8 wt% Si and 0.4 wt% Co. This alloy was selected for three reasons: (i) the basic mechanical properties [14, 15] and fracture characteristics [16] of this material have been established in earlier investigations, (ii) the alloy is essentially single-phase but contains a uniform dispersion of a Co-rich phase which may act as effective pinning points for intragranular dislocations and thereby assist the microstructural examinations, and (iii) the sliding contributions reported to date are generally for materials exhibiting high superplasticity and stress exponents close to 2 in Region II, whereas the selected alloy exhibits only rather modest elongations to failure (up to ~380% [16]) and a correspondingly higher stress exponent of $n \simeq 2.8$ [14] in Region II.

## 2. Experimental procedure

Hot-rolled sheets of Coronze CDA 638 were obtained with a thickness of 1.3 mm. The initial spatial grain sizes, $d$, were either 3.0 or 7.0 $\mu$m, where $d$ is defined as $1.74 \times \bar{L}$ where $\bar{L}$ is the mean linear intercept. Tensile specimens, having a gauge length of 2.54 cm, were cut from the sheets with the tensile axis parallel to the rolling direction. Prior to testing, some specimens having a grain size of 7.0 $\mu$m were annealed in argon for 3 days at 833 ± 1 K to give a grain size of $d = 7.9\,\mu$m. The accuracy of the grain-size measurements was ± 10%.

For the transmission electron microscopy, specimens were tested in air under creep conditions using a creep machine with a contoured lever arm to maintain conditions of constant stress. Testing temperatures of either 723 or 823 K were maintained constant to within ±1 K using a three-zone vertical tube furnace and a proportional temperature controller. The strain was monitored continuously using a linear variable differential transformer and recorded using an amplifier and strip-chart recorder. The accuracy of the strain measurements was $\pm 4 \times 10^{-5}$.

Two types of creep test were conducted. Initially, several specimens were deformed at constant stress levels to provide reasonably complete plots of strain against time. Subsequently, additional specimens were deformed to some point within the steady-state region and then cooled very rapidly under load. An air blower was used to increase the cooling rate after the furnace was removed.

Two different procedures were employed to prepare foils for transmission electron microscopy. In the first method, sections from the specimen gauge length were ground carefully to ~0.15 mm thickness and then thinned by electropolishing at a temperature below −25° C in a solution of 33 vol% nitric acid and 67 vol% methanol. A stainless-steel cathode was used and the bath was continuously agitated with a glass rod. A window technique was adopted in which the edges of the sample were painted with a protective lacquer and the thinning process was terminated at the point of perforation. The specimen was then removed quickly from the electrolyte and rinsed in methanol. In the second method, which was used as a precautionary check to ensure that no damage was introduced by the preparation procedure, the sample was ground to ~0.25 mm thickness and then polished chemically to ~0.05 mm thickness in a solution of 30 vol % $HNO_3$, 10 vol % HCl, 10 vol % $H_3PO_4$ and 50 vol % acetic acid at 75° C. Thereafter, a thin foil was prepared using the same electropolishing technique. A detailed examination of the thin foils in the electron microscope revealed no obvious differences between these two preparation procedures.

For the measurements of grain-boundary sliding, specimens having a grain size of 7.9 $\mu$m were tested at 823 K on an Instron machine operating at a constant rate of cross-head displacement. Prior to testing, each specimen was carefully polished on a range of silicon carbide papers and on 6 and 1 $\mu$m diamond pastes and then a very smooth surface was obtained by electropolishing in 33 vol % nitric acid and 67 vol % methanol. Scratches were carefully placed on the specimen surface, parallel to the tensile axis, using 0.25 $\mu$m diamond paste on a tissue. To preserve the highly-polished surface

and minimize oxidation, each specimen was tested in an atmosphere of pre-purified argon. The tests were terminated at an elongation of 10% and the specimens were then removed from the testing machine and examined using scanning electron microscopy.

The extent of grain-boundary sliding was estimated by taking a series of measurements of the offset, $w$, occurring at each grain boundary intersected by a longitudinal marker line and the associated angle, $\theta$, between the trace of the boundary in the plane of the surface and the stress axis.

## 3. Experimental results

### 3.1. Mechanical properties

Typical creep curves are shown in Fig. 1 for specimens having a grain size of 7.9 $\mu$m tested at an absolute temperature, $T$, of 823 K, plotted as strain $\epsilon$, against time, $t$. It should be noted that, for convenience of presentation, the time scale is in minutes for the two tests conducted at 66.2 and 29.9 MN m$^{-2}$ and in hours for the test at 10.1 MN m$^{-2}$: these three stress levels correspond to Regions III, II and I, respectively [14]. As noted earlier [14], there is only a very brief primary stage of creep in Regions I and II, but the primary stage is significantly longer in Region III.

When plotted in the form of steady-state strain rate against stress, the datum points from both creep (constant stress) and Instron (nominally constant strain rate) tests tend to superimpose and lie along a well-defined sigmoidal curve [14]. This is illustrated schematically in Fig. 2: complete details of the mechanical data were presented earlier [14]. The horizontal arrows in Fig. 2 indicate the three strain rates selected to deform specimens for measurements of grain-boundary sliding in Regions I, II and III.* The vertical arrows show the three stress levels selected for creep experiments and subsequent examination by transmission electron microscopy.

### 3.2. Microstructural observations

The microstructure of an annealed specimen prior to testing is shown in Fig. 3. This sample, having a grain size of 3.0 $\mu$m, shows an aggregate of essentially equiaxed grains, a random dispersion of a very fine cobalt-rich precipitate throughout the grains and a fairly high density of twins. Fig. 3 is typical of the microstructure of this alloy in the annealed condition. After deformation, the microstructures tended to be rather inhomogeneous: the results presented in this section represent an attempt to provide reasonably general observations.

Figs 4 to 6 give typical microstructures of specimens with a grain size of 7.9 $\mu$m deformed to a total strain of 10% at 823 K in Regions III, II and I, respectively.

Fig. 4, obtained at 71.7 MN m$^{-2}$ in Region III, shows the presence of many tangled dislocations within the central grain. In general, it was found that some grains contained a high density of dislocations which were fairly uniformly distributed and other grains contained heavily tangled dislocations. No subgrain formation was observed in Region III in specimens deformed either at 823 or 723 K, and the general appearance of the grains

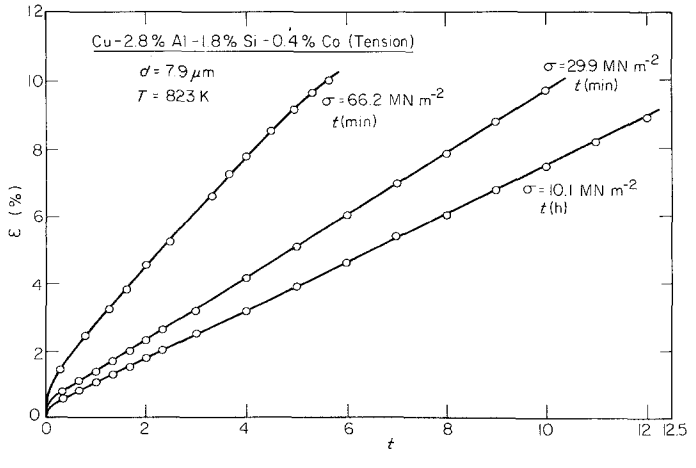


*Figure 1* Creep strain against time for three specimens tested at different stress levels at a temperature of 823 K.

*The lowest horizontal arrow lies only just within Region I: this point, corresponding to a strain rate of $3.33 \times 10^{-6}$ sec$^{-1}$, represents the lowest rate available on the Instron machine for the present experimental conditions.

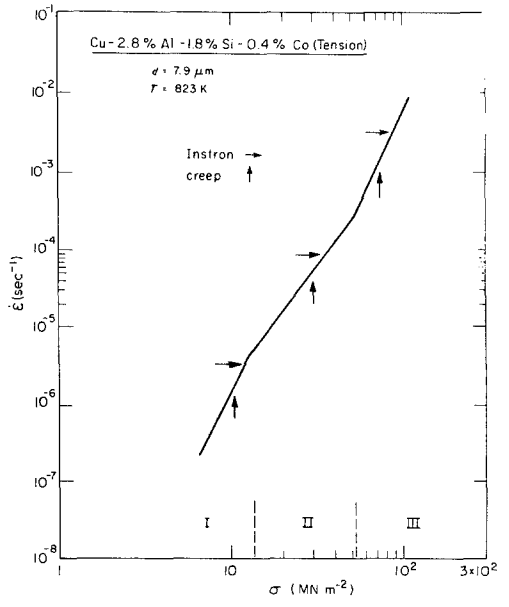


*Figure 2* Strain rate against stress for a grain size of 7.9 $\mu$m at 823 K: the arrows indicate selected strain rates and stresses for subsequent experiments.

was similar at both temperatures. The lack of subgrain formation was confirmed by deforming a specimen, having a grain size of 7.0 $\mu$m, at a stress of 104.1 MN m$^{-2}$ to a strain of 50% in Region III: this specimen again contained many dislocation tangles but no eividence of subgrain boundaries.

Fig. 5 was obtained in Region II at a stress of 29.9 MN m$^{-2}$. The microstructures observed in this region were very different to those in Region III. In general, the dislocation density was low and many grains appeared to be dislocation-free. No dislocation tangles were visible in any of the grains of specimens examined in Region II and many of of intragranular dislocations tended to be associated with precipitates. Some widely dissociated dislocations were observed in some grains due to the low stacking-fault energy of the alloy. In addition, long dislocation pile-ups, containing up to ~30 dislocations, were observed occasionally in a very small number of the grains.

Fig. 6 shows a typical microstructure after deformation in Region I at 10.1 MN m$^{-2}$. As in Region II, no dislocation tangles were visible, many grains were apparently dislocation-free and most of the dislocations appeared to be pinned at precipitates. Two specimens having a grain size of 3.0 $\mu$m were deformed in Region I to strains of 8.6 and 22% at a temperature of 723 K and stresses of 26.5 and 30.1 MN m$^{-2}$, respectively. Both specimens exhibited similar microstructures with relatively few intragranular dislocations, although there was some evidence of grain growth in the specimen deformed to the higher strain.

## 3.3. Measurements of grain boundary offsets

As indicated in Fig. 2, specimens having a grain size of 7.9 $\mu$m were tested on an Instron machine at 823 K at initial strain rates of $3.33 \times 10^{-3}$ sec$^{-1}$ (Region III), $8.33 \times 10^{-5}$ sec$^{-1}$ (Region II) and $3.33 \times 10^{-6}$ sec$^{-1}$ (Region I). Each specimen was taken to a strain of 10% and the appearances of the surfaces after deformation are shown in the scanning electron micrographs in Figs 7 to 9. In each case, the tensile axis is horizontal and some longitudinal surface marker lines are clearly visible.

In Region III, the surface was disturbed and very irregular, as shown in Fig. 7, suggesting the

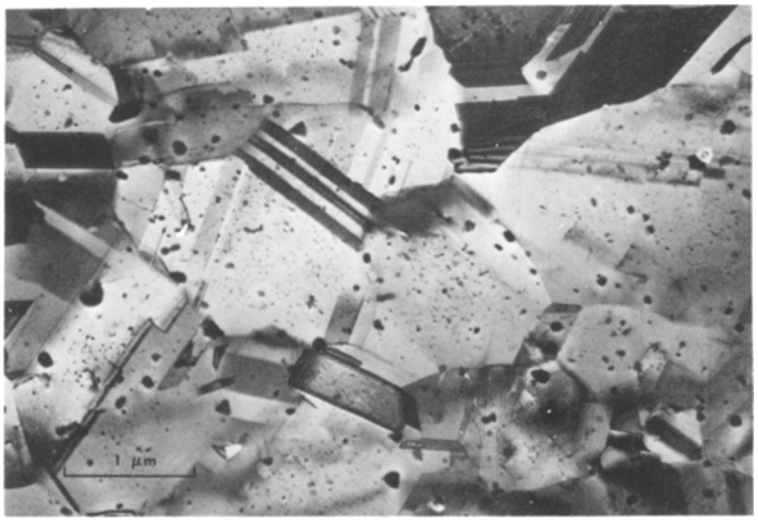


*Figure 3* The microstructure of an annealed specimen prior to testing.

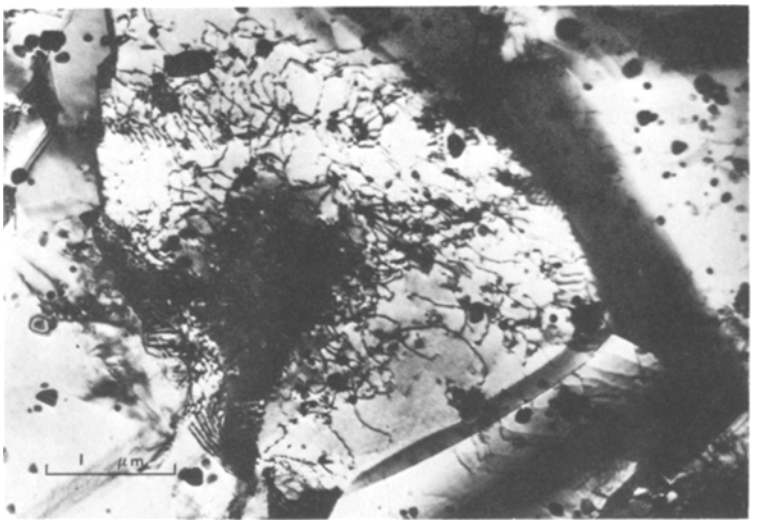


*Figure 4* The microstructure of a specimen deformed to 10% at 823 K in Region III.

occurrence of extensive slip within the grains and especially in the vicinity of many of the boundaries. The offsets due to grain-boundary sliding were relatively small in this region and the average offset, $\bar{w}$, was only 0.060 $\mu$m from a total of 300 individual readings.

There was extensive grain-boundary sliding and obvious grain rotation in the specimen deformed in Region II. The surface remained relatively flat in this region, although there was clear evidence at many boundaries of a displacement due to sliding perpendicular to the surface. In addition, there was some evidence of cavity formation at the surface, thereby confirming earlier observations of extensive internal cavitation in this alloy [16]. A large offset in a marker line at a grain boundary almost perpendicular to the stress axis is shown in Fig. 8: in examples of this type, the magnitude of the offset was recorded by projecting the marker line across the interface to give the total displacement perpendicular to the stress axis. For this specimen, the average offset from 350 readings of $w$ was 0.133 $\mu$m.

It was difficult to take measurements of $w$ in Region I because the marker lines tended to become diffuse, probably due to the long testing time. An example is shown in Fig. 9. As in Region II, the surface remained relatively flat and there was again some surface evidence for cavity formation. The amount of sliding in this region was less than in Region II and the average offset from 110 measurements of $w$ was 0.085 $\mu$m.

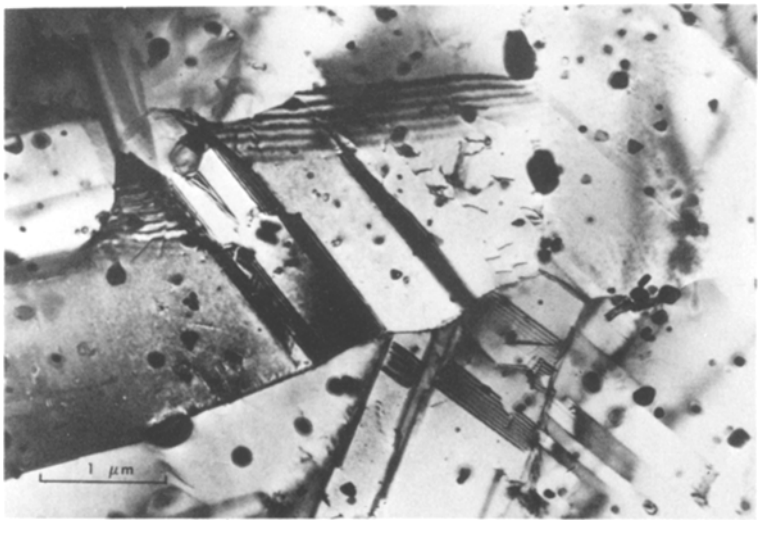


*Figure 5* The microstructure of a specimen deformed to 10% at 823 K in Region II.

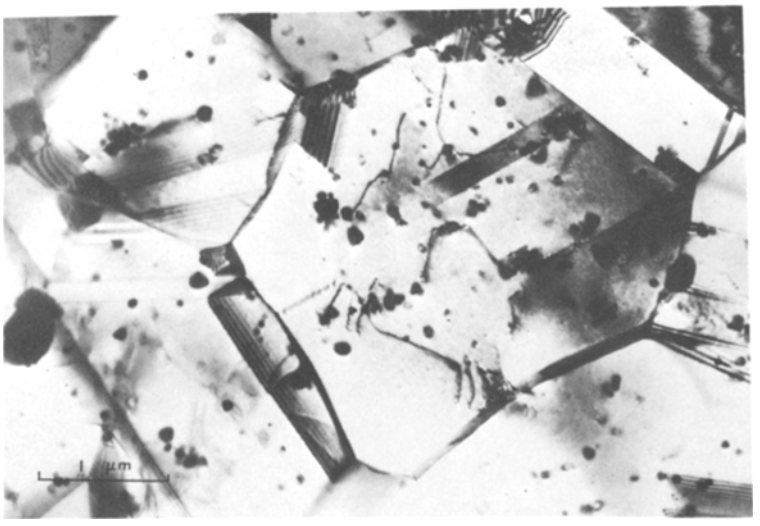

*Figure 6* The microstructure of a specimen deformed to 10% at 823 K in Region I.

## 4. Discussion

### 4.1. The magnitude of grain-boundary sliding

The measurements of the offsets in marker lines were used to determine the magnitude of the strain due to grain-boundary sliding, $\epsilon_{gbs}$. Two different procedures were used for these calculations.

First, $\epsilon_{gbs}$ was estimated from the expression [17]

$$\epsilon_{gbs} = \frac{\phi \bar{w}_1}{\bar{L}}, \qquad (1)$$

where $\phi$ is a geometrical constant which relates the average transverse offset to a normal strain along the tensile axis and the subscript "1" denotes the procedure of taking measurements along a longitudinal marker line. Previous evaluations under creep conditions have given values of $\phi$ of 1.62 and 1.44 from theoretical and experimental approaches, respectively [17]. Thus, following the standard procedure adopted for creep [18], $\phi$ was put equal to 1.5.

Second, $\epsilon_{gbs}$ was estimated from the equation [18]

$$\epsilon_{gbs} = \frac{2\overline{(w/\tan\theta)}_1}{\bar{L}}, \qquad (2)$$

where $\overline{(w/\tan\theta)}_1$ refers to the average value of $(w/\tan\theta)$ determined from a series of measurements of $w$ and $\theta$ at the grain boundaries intersected by a longitudinal marker line.

Equation 2 is an exact relationship for $\epsilon_{gbs}$ and Equation 1 is a simplification: the factor of 2 in Equation 2 is due to the necessity to allow for equal displacements perpendicular to the surface [19].

Table I gives the values obtained for $\epsilon_{gbs}/\epsilon_t$ as

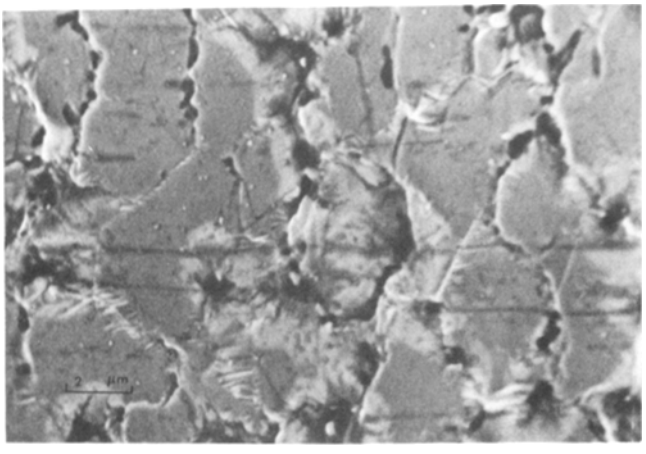

*Figure 7* The surface of a specimen deformed to 10% at 823 K in Region III: the tensile axis is horizontal.

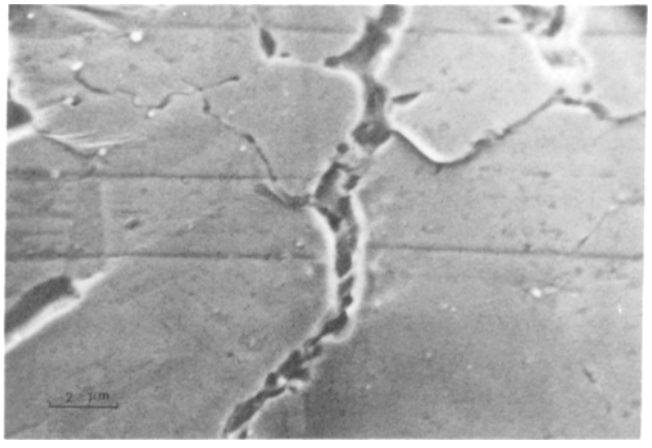


*Figure 8* The surface of a specimen deformed to 10% at 823 K in Region II: the tensile axis is horizontal.

a percentage in the three regions of flow, where $\epsilon_t$ is the total strain (equal to 10% in these experiments). These values show two important trends. First, maximum sliding occurs in the superplastic Region II and there is a decrease in the less superplastic Regions I and III: this is similar to the results reported for a number of different superplastic materials [13]. Second, there is a consistent difference in the results obtained using Equations 1 and 2, such that the values of $\epsilon_{gbs}/\epsilon_t$ tend to be slightly lower when calculated from Equation 2. The reason for this difference is not clear, although it probably arises because of the very small grain size which makes it extremely difficult to obtain accurate values of $\theta$. Reference to Figs 7 to 9 shows that $\theta$ may tend to be overestimated by assuming that the boundaries are more nearly perpendicular to the tensile axis. This effect would lead to an overestimation of $\tan\theta$ and a consequent erroneous reduction in the value estimated for $\epsilon_{gbs}$ from Equation 2. In the circumstances, it is believed that the most reliable values of $\epsilon_{gbs}/\epsilon_t$ are obtained from Equation 1.

It is interesting to note that the value of $\epsilon_{gbs}/\epsilon_t = 44 \pm 10\%$ in Region II is slightly lower than the values of 50 to 70% reported in many experiments [13], although the difference may not be significant because of the large associated error bar. However, most of the earlier experiments were conducted on superplastic metals having a stress exponent close to 2 in Region II, although Valiev and Kaibyshev [20] obtained $\epsilon_{gbs}/\epsilon_t = 49 \pm 6\%$ in Region II in an Mg–1.5 wt% Mn–0.3 wt% Ce alloy containing Mn precipitates. The latter material gave a stress exponent of $n \simeq 2.6$ at the strain rate where the sliding measurements were taken [20] and this is comparable to the value of $n = 2.8$ obtained in Region II for the present alloy [14]. Thus, it appears that the stress exponent tends to be higher in Region II in the less superplastic alloys containing precipitates and this leads to lower elongations to falure under optimum

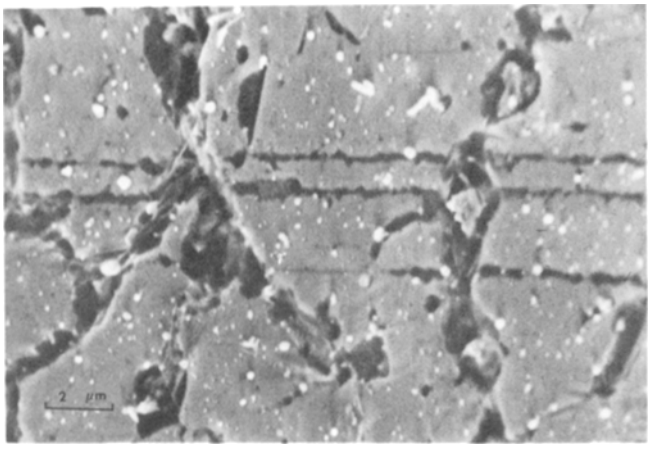


*Figure 9* The surface of a specimen deformed to 10% at 823 K in Region I: the tensile axis is horizontal.

TABLE I Values obtained for $\epsilon_{gbs}/\epsilon_t$ in Regions III, II and I

| Region | Equation 1 | Equation 2 |
|---|---|---|
| III | 20 ± 5% | 14 ± 4% |
| II | 44 ± 10% | 39 ± 9% |
| I | 28 ± 12% | 18 ± 8% |

superplastic conditions* and a corresponding decrease in the contribution of grain-boundary sliding. It seems likely also that the presence of precipitates at the grain boundaries may contribute to the decrease in magnitude of sliding in Region II in these less superplastic alloys.

## 4.2. Microstructural observations

The present observations in Regions II and III are similar to earlier reports on other superplastic alloys of extensive dislocation activity in Region III and only limited dislocation activity in Region II [7, 9, 10].

The stress exponent in Region III is 4.7 [14] and this suggests the occurrence of a dislocation creep process such as dislocation climb. No subgrains were observed in this region, but this is consistent with an estimate of the anticipated subgrain size at this stress level. Under creep conditions in non-superplastic metals, the average subgrain size, $\lambda$, is given by [23]

$$\frac{\lambda}{\mathbf{b}} = 20\left[\frac{\sigma}{G}\right]^{-1}, \qquad (3)$$

where $\mathbf{b}$ is the Burgers vector and $G$ is the shear modulus. Putting $\mathbf{b} = 2.56 \times 10^{-10}$ m for Cu and taking the shear modulus for this alloy at an absolute temperature, $T$, as [14]

$$G = (4.80 \times 10^4 - 1.77\,T)\,\mathrm{MN\,m^{-2}}, \qquad (4)$$

the average subgrain size is estimated as $\lambda \simeq 3.3\,\mu$m. This is equivalent to a spatial subgrain size, $\lambda_s$, of $1.74 \times 3.3 \simeq 5.7\,\mu$m, which is of the order of the spatial grain size of $d = 7.9\,\mu$m. Thus, the stable subgrain size is similar in magnitude to the grain size and no subgrain boundaries would be observed under these conditions.

The experimental evidence, as exemplified by Fig. 4, suggests that deformation in Region III occurs primarily by an intragranular dislocation creep mechanism. However, it was reported earlier that there is a significant dependence on grain size in Region III, such that the creep rate is inversely proportional to the grain size raised to a power of 1.2 [14]. This earlier observation is consistent both with the presence of some grain-boundary sliding in this region, as indicated in Table I, and the observations, as in Fig. 7, of extensive deformation in the boundary regions. It is therefore concluded that Region III is due to intragranular dislocation creep accompanied by some grain-boundary sliding which is accommodated by local dislocation movement in the vicinity of the grain boundaries.

Intragranular dislocation creep becomes of less importance as the stress level is reduced to Region II, as indicated in Fig. 5, but there is also a corresponding increase in the importance of grain-boundary sliding. Many of the dislocations observed in this region appeared to be associated with precipitates and this is consistent with observations in the Al-rich grains of the Zn–22 wt % Al eutectoid [24]. As noted by Valiev *et al.* [12], a series of randomly dispersed precipitates are probably necessary to hold up dislocations which would otherwise easily disappear into the grain boundaries during post-testing cooling and unloading. The present observation that dislocation pile-ups occur only in a very few grains in Region II is identical to an earlier report on Zn–22 wt % Al by Misro and Mukherjee [25]. Thus, the evidence in Region II suggests deformation by a combination of grain-boundary sliding and some intragranular slip.

The observations in Region I reveal very little dislocation activity and the few dislocations visible in the electron microscope usually appear to be held up at precipitates. There is a decrease in the magnitude of grain-boundary sliding in this region but there appears to be no concomitant increase in the extent of intragranular slip. This observation therefore contrasts with the report by Kaibyshev *et al.* [10] on various Zn–Al alloys, in which it was concluded that the transition from Regions I to II corresponded to a transition from single to multiple slip and that the slip contribution reached a minimum of ~ 20% in Region II and increased at both higher and lower strain rates. More experimental work is required on other superplastic alloys in Region I to resolve this apparent dichotomy.

*Compare, for example, the optimum elongation of 380% in the present alloy with $n = 2.8$ [16] and the elongation of 2900% in Zn–22 wt % Al with $n = 2.0$ [21] and 4850% in Pb–62 wt % Sn with $n = 1.6$ [22].

Finally, it should be noted that some theories of superplasticity attribute Region I to the presence of a threshold stress [26, 27], but this concept is not consistent with the present results because it fails to explain the very marked decrease in $\epsilon_{gbs}/\epsilon_t$ in Region I. In fact, no theory is at present available which accounts for a decrease in the sliding contribution at very low strain rates. In summary, therefore, the present observations indicate that Region I is due to a combination of grain-boundary sliding, a small amount of intragranular slip and some associated, and as yet unidentified, additional process which, based on earlier evidence [15], is diffusion-controlled.

## 5. Summary and conclusions

(1) There are significant differences in the microstructures of specimens of a superplastic Cu alloy deformed in the three regions of plastic flow. At high strain rates in Region III, there is extensive dislocation activity and many heavily tangled dislocations. At intermediate and low strain rates in Regions II and I, the dislocation density is low and many grains appear to be dislocation-free.

(2) Grain-boundary sliding is important in Region II and the strain contributed by sliding is slightly under 50% for the testing conditions used in these experiments. There is a significant decrease in the sliding contributions in the less superplastic Regions I and III.

## Acknowledgements

We are grateful to Dr E. Shapiro of the Olin Corporation for supplying the material used in this investigation. This work was supported by the National Science Foundation under Grant No. DMR79–25378.

## References

1. J. W. EDINGTON, K. N. MELTON and C. P. CUTLER, *Prog. Mater. Sci.* **21** (1976) 61.
2. D. M. R. TAPLIN, G. L. DUNLOP and T. G. LANGDON, *Ann. Rev. Mater. Sci.* **9** (1979) 151.
3. H. NAZIRI, R. PEARCE, M. HENDERSON BROWN and K. F. HALE, *J. Microsc.* **97** (1973) 229.
4. H. NAZIRI, R. PEARCE, M. HENDERSON BROWN and K. F. HALE, *Acta Met.* **23** (1975) 489.
5. R. H. BRICKNELL and J. W. EDINGTON, *ibid.* **25** (1977) 447.
6. R. C. GIFKINS, *J. Mater. Sci.* **13** (1978) 1926.
7. L. C. A. SAMUELSSON, K. N. MELTON and J. W. EDINGTON, *Acta Met.* **24** (1976) 1017.
8. K. MATSUKI, Y. UETANI, M. YAMADA and Y. MURAKAMI, *Metal Sci.* **10** (1976) 235.
9. R. Z. VALIEV and O. A. KAIBYSHEV, *Phys. Stat. Sol. (a)* **44** (1977) 477.
10. O. A. KAIBYSHEV, B. V. RODIONOV and R. Z. VALIEV, *Acta Met.* **26** (1978) 1877
11. K. MATSUKI, K. MINAMI, M. TOKIZAWA and Y. MURAKAMI, *Metal Sci.* **13** (1979) 619.
12. R. Z. VALIEV, O. A. KAIBYSHEV, M. M. MYSHLAYEV and D. R. CHALAEV, *Scripta Met.* **14** (1980) 673.
13. T. G. LANGDON, *J. Mater. Sci.* **16** (1981) 2613.
14. S.-A. SHEI and T. G. LANGDON, *Acta Met.* **26** (1978) 639.
15. *Idem, ibid.* **26** (1978) 1153.
16. *Idem, J. Mater. Sci.* **13** (1978) 1084.
17. R. L. BELL, C. GRAEME-BARBER and T. G. LANGDON, *Trans. AIME* **239** (1967) 1821.
18. T. G. LANGDON, *Met Trans.* **3** (1972) 797.
19. R. L. BELL and T. G. LANGDON, *J. Mater. Sci* **2** (1967) 313.
20. R. Z. VALIEV and O. A. KAIBYSHEV, *Phys. Stat. Sol. (a)* **44** (1977) 65.
21. H. ISHIKAWA, F. A. MOHAMED and T. G. LANGDON, *Phil. Mag.* **32** (1975) 1269.
22. M. M. I. AHMED and T. G. LANGDON, *Met. Trans. A* **8A** (1977) 1832.
23. J. E. BIRD, A. K. MUKHERJEE and J. E. DORN, "Quantitative Relation Between Properties and Microstructure," edited by D. G. Brandon and A. Rosen (Israel Universities Press, Jerusalem, 1969) p. 255.
24. T. G. LANGDON and F. A. MOHAMED, Proceedings of the 4th International Conference on the Strength of Metals and Alloys, Vol. 1 (Laboratoire de Physique du Solide, ENSMIM, Nancy, France, 1976) p. 428.
25. S. C. MISRO and A. K. MUKHERJEE, "Rate Processes in Plastic Deformation of Materials," edited by J. C. M. Li and A. K. Mukherjee (American Society for Metals, Metals Park, Ohio, 1975) p. 434.
26. M. F. ASHBY and R. A. VERRALL, *Acta Met.* **21** (1973) 149.
27. J. H. GITTUS, *J. Eng. Mater. Technol.* **99** (1977) 244.

Received 16 February and accepted 26 March 1981.